SJSS
SPANISH JOURNAL OF SOIL SCIENCE

# Paleoclimatic implications of micromorphic features of a polygenetic soil in the Monegros Desert (NE-Spain)

*Implicaciones paleoclimáticas de los rasgos micromorfológicos de un suelo policíclico en el Desierto de Monegros (NE-España)*
*Implicações paleoclimáticas das características micromorfológicas de um solo policíclico no Deserto de Monegros (NE-Espanha)*

AUTHORS

**Badía D.**[@ 1]
badia@unizar.es

**Poch R.M.**[2]

**Martí C.**[1]

**García-González M.T.**[3]

[@] Corresponding Author

[1] Technic School of Agrarian Engineering and Environmental Sciences, University of Zaragoza. Huesca, Spain.

[2] Departament de Medi Ambient i Ciències del Sòl. ETSEA, Universitat de Lleida. Rovira Roure 191. 25198 Lleida, Spain.

[3] Instituto de Ciencias Agrarias, Consejo Superior de Investigaciones Científicas. C/Serrano, 115 dup. 28006 Madrid, Spain.

**Received:** 11.12.2012 | **Revised:** 09.04.2013 | **Accepted:** 22.05.2013

## ABSTRACT

Pedofeatures can be repositories of information about soil forming factors such as climate. The aim of this work is to provide a model of interpretation of a polygenetic soil in the Monegros desert (Ebro Basin, NE-Spain) and its relationship to environmental changes during the Quaternary. To achieve this goal, the physical, chemical, mineralogical and especially the micromorphic pedofeatures of this profile were studied. Carbonate accumulations extend into all of the horizons of the profile. The paleosol has a thick petrocalcic horizon at the top, with a massive-laminar structure comprising layers of micrite and sparite that sometimes form pendants. Towards its base, the petrocalcic horizon contains a spaced framework of orthic micrite nodules packed between relatively pure micritic laminar bands. Below the petrocalcic horizon, coatings and infillings of microcrystalline calcite occur in old channels, and soft concretions (some of them geodic) indicate an in situ accumulation process (Bkc, calcic horizon). Another calcic horizon with orthic nodules of calcite, impregnative and diffuse (Ckc), is present at the bottom part of the profile. Between the two nodular calcic horizons, two recarbonated argic horizons are found (Btkc and Btk) with coarse orthic nodules of dense micrite superimposed on textural pedofeatures. These textural micromorphic pedofeatures are: (1) interbedded microlaminated clay pockets not associated with current or past pores and (2) microlaminated clay and silt (dusty clay) present as weakly oriented coatings on channel walls. Reduction pedofeatures are associated with textural ones: (1) coatings of manganese oxides around pore channels and cracks, and (2) nodules of manganese and iron oxides within the peds. The presence of calcic horizons alternating with argic horizons, all positioned below the petrocalcic horizon, confirm fluctuations in paleohydrological conditions in the Pleistocene. Its presence indicates that the oldest soil corresponds to a Calcic Luvisol-like pedotype, which is overlain by an Haplic Calcisol-like pedotype and this, in turn, by a Petric Calcisol-like pedotype. This superposition of profiles indicates, within the mentioned climatic changes, a tendency towards increasing dryness during the Pleistocene in the semiarid Ebro Valley.

DOI: 10.3232/SJSS.2013.V3.N2.06

SJSS
SPANISH JOURNAL OF SOIL SCIENCE

**RESUMEN**

*Los edaforrasgos son el resultado de procesos y factores de formación, por lo que su presencia nos da información sobre los cambios ambientales que han tenido lugar con la evolución del suelo. El objetivo de este trabajo es proporcionar un modelo de interpretación de un suelo policíclico en el Desierto de Monegros (Cuenca del Ebro, NE-España) y relacionarlo con los cambios ambientales a lo largo del Cuaternario. Para lograr este objetivo se describen las propiedades físicas, químicas, mineralógicas y micromorfológicas de este perfil. La carbonatación es evidente en todos y cada uno de los horizontes del perfil. En la parte superior, un grueso horizonte petrocálcico presenta una estructura laminar con capas de micrita y esparita, que a veces forman pendents. Hacia su base, estas capas laminares relativamente puras, micríticas, se intercalan con nódulos órticos de micrita. Por debajo del horizonte petrocálcico aparecen revestimientos y rellenos de calcita microcristalina en antiguos canales junto a nódulos blandos, geódicos (horizonte cálcico, Bkc), registro de un proceso de acumulación in situ. Otro horizonte con nódulos órticos de calcita, impregnativos y difusos se describen en la parte inferior del perfil (Ckc). Entre ambos horizontes cálcicos nodulares se encuentran horizontes árgicos recarbonatados con gruesos nódulos órticos de micrita densa, superpuestos a edaforrasgos texturales (Btkc y Btk). Los microedaforrasgos texturales encontrados en el horizonte árgico son de dos tipos: (1) intercalaciones de arcilla laminada en paquetes, no asociadas con poros actuales o pasados y (2) microlaminaciones de arcilla y limo recubriendo las paredes de poros, orientados débilmente. Asociados a estos rasgos texturales aparecen edaforrasgos de reducción: (1) hipo y cuasi-revestimientos de óxidos de manganeso alrededor de canales de poros y grietas, y (2) nódulos dendríticos, de óxidos de manganeso y hierro, dentro de agregados. La combinación de los edaforrasgos y horizontes descritos permiten clasificar el suelo más antiguo como un Luvisol cálcico, sobre el que se desarrolló un Calcisol háplico, ambos sellados por un Calcisol pétrico. Esta secuencia de perfiles es una evidencia de fluctuaciones en las condiciones paleohidrológicas a lo largo del Pleistoceno, combinada con una creciente aridez en el semiárido Valle del Ebro.*

**RESUMO**

*Algumas edafocaracteristícas constituem repositórios de informação sobre os factores de formação do solo, como é o caso do clima. O objectivo deste estudo é propor um modelo de interpretacão de um solo policíclico no Deserto de Monegros (Bacia do Ebro, NE-Espanha) e relacioná-lo com as alterações ambientais durante o Quaternário. Para atingir este objetivo descrevem-se as propriedades físicas, químicas, mineralógicas e em especial as micromorfológicas dos horizontes deste perfil. A carbonatacão é bem evidente em todos os horizontes do perfil. Na parte superior do solo policíclico, surge um espesso horizonte petrocálcico apresentando uma intensa estrutura laminar com lâminas de micrite e esparite, que por vezes formam pendentes. O horizonte Petrocálcico, apresenta na sua base espaçadamente nódulos de micrite relativamente puros intercalados entre lâminas de micrite. Abaixo do horizonte petrocálcico, ocorrem revestimentos e incrustações de calcite microcristalina em canais antigos e concreções macias (alguns deles, geodicos) indiciando um processo de acumulação in situ (Bkc, horizonte cálcico). Um outro horizonte cálcico com nódulos de calcite impregnativos e difusos (Ckc), surge na parte inferior do perfil. Entre ambos os horizontes cálcicos nodulares, encontram-se dois horizontes árgicos recarbonatados (Btkc e Btk) com nódulos órticos grosseiros de micrite densos sobrepostos, nas pedocaracterísticas texturais. Estas pedocaracterísticas micromórficas texturais são: (1) bolsas de argila microlaminadas incrustadas na sua base, não associadas a poros atuais ou antigos (2) microlâminas de argila e limo recobrindo as paredes de poros, fracamente orientadas. Asociadas a estas características texturais aparecem edafocaracterísticas de redução: (1) hipo e quase-revestimentos de óxidos de manganês em redor de canais de poros e fendas (2) nódulos dendritícos de óxidos de manganês e ferro dentro de agregados. A combinação das edafocaracterísticas e horizontes descrito permitem clasificar o solo mais antigo como um Luvisol cálcico sobre o qual se desenvolvou um Calcisol háplico, ambos selados por um Calcisol pétrico. Esta sequência de perfis é uma evidencia de flutuações nas condições paleohidrológicas ao longo do Pleistocénico, asociada a uma crescente aridez, no semiárido vale do Ebro.*

**KEY WORDS**
**Micromorphology, carbonate accumulations, hydromorphic pedofeatures, textural pedofeatures, clay mineralogy; Pleistocene, Ebro Basin**

**PALABRAS CLAVE**
Micromorfología, carbonatación, rasgos hidromorfos, edaforrasgos texturales, mineralogía de las arcillas, Pleistoceno, Valle del Ebro

**PALAVRAS-CHAVE**
Micromorfologia, carbonatacão, caracteristícas hidromórficas, edafocaracteristícas texturais, mineralogía das argilas, Pleistoceno, Valle del Ebro

# 1. Introduction

During the Quaternary, the landscape has been subjected to a wide variation of environmental conditions which have left distinct footprints in soils as a result of past processes. This is the case of polygenetic or polycyclic soils, a composite of horizons from more than one soil-forming event (Chesworth 2008; Fedoroff et al. 2010). Polygenetic soils can be also considered a complex of soils formed in pre-Holocene environments different from today, subsequently subjected to processes of burial by younger sediments and exhumation by erosion (Nettleton et al. 2000). The study of paleosols is a tool in the reconstruction of the paleoclimate and regional landscape dynamics on the basis of the processes inferred from soil properties (Hamer et al. 2007; Brock and Buck 2009; Markovic et al. 2011). Paleopedology is a useful proxy to reconstruct paleoenvironmental conditions but is still an immature field (Sheldon and Tabor 2009). Moreover, there are few studies on paleopedogenic processes in semiarid Mediterranean regions because the soils are generally weakly developed and rarely preserved due to low plant cover and high erosion rates (Zielhofer et al. 2009).

The Ebro Basin, the northernmost semiarid region in Europe, is an area with high sensitivity to environmental changes that contains excellent morphosedimentary records of Quaternary climate oscillations (Lewis et al. 2009; Sancho et al. 2011). Previous research on paleoenvironmental and paleoclimatic reconstruction in continental deposits of Ebro Basin has been focused on sedimentological and paleontological studies (González-Sampériz et al. 2010; Sancho et al. 2011; Moreno et al. 2012). However, the significant wealth of information that can be acquired from processes in paleosols from semiarid regions is only now starting to come to light (Hamer et al. 2007; Brock and Buck 2009; Meléndez et al. 2011). In this sense, some soil processes such as secondary carbonate precipitation and clay illuviation can be repositories of information about past soil forming factors (Brock and Buck 2009). Petrocalcic horizons (calcrete, also known by popular names such as caliche, mallacán, calicanto, cervell de gat, etc.) are very frequent in semiarid regions such as the Ebro Basin, forming on old stable surfaces where soils display progressive and systematic patterns of carbonate accumulation over time (Gómez-Miguel 2005; Sancho et al. 2008; Lewis et al. 2009). Although petrocalcic formation has generally been understood to be a continuous process with no interruptions by sedimentation or erosion (Gile et al. 1966; Machette 1985; Nettleton et al. 1991), non-linear models have also been proposed (Huggett 1998; Meléndez et al. 2011). In calcretes evolved on Early Pleistocene terraces of the Segre River, a tributary of the Ebro, alternating layers of carbonates and illuvial clay provide unequivocal evidence of the various phases of successive secondary carbonate precipitation, and it has been interpreted as the reflex of climatic changes during the Quaternary (Badía et al. 2009a). Beside carbonation, clay illuviation is another common pedofeature in semiarid to subhumid regions in relatively stable landforms (Dorronsoro and Alonso 1994; Khormali et al. 2003; Ortiz et al. 2002; Roquero et al. 1999; Dan et al. 1981). However, Nettleton et al. (2000) suggested that smectitic argillic horizons in the Argid sub-order (Soil Survey Staff 2010) are Pleistocene relicts related to a wetter climate. Clay translocation, also called argilluviation or lessivage, is traditionally considered to be promoted by a low organic matter content, coarse to medium textured soils, a smectite-dominated clay fraction and, especially, a soil pH of 5.5 to 6.5 with no $Ca^{2+}$, $Mg^{2+}$ or $Al^{3+}$ to act as binding agents (Khormali et al. 2003; Chesworth 2008; Quénard et al. 2011). Therefore, decarbonation and desaturation seem to be preliminary steps to clay transfer from an elluvial horizon to an illuvial one, although Poch et al. (2012) suggested that spatial differentiation of soil environments in the profile could allow the temporal coexistence of clay illuviation and calcification.

The aim of this work is to provide a model of a polycyclic soil in the Monegros desert (Ebro Basin, NE-Spain) which formed during the Pleistocene. To achieve this goal, the physical, chemical, mineralogical, and morphological properties of this complex profile were studied. Particular emphasis is placed on the micromorphology, particularly calcification and textural pedofeatures, and its relationship to environmental changes.

# 2. Materials and Methods

## 2.1. Geologic setting and background

The studied paleosol was sampled in cliff edges of the Saso (= mesa) de las Fitas landform (**Figure 1**), near the village of Sariñena (Monegros county, NE-Spain). The region has a semi-arid Mediterranean climate, with a mean annual precipitation (MAP) about 400 mm and a mean annual temperature (MAT) of 14.5 °C; the ratio of rainfall to mean annual reference crop evapotranspiration (P/ETo) is about 0.35. The paleosol is placed at the north-central Tertiary Ebro Basin, the southern foreland basin of the Pyrenean mountain range. The sedimentary regime of this Basin persisted until the end of the late Miocene (between 12.5 and 8.5 Ma) when the internal drainage opened due to aggradation of lacustrine environments and extension into the western Mediterranean basin (García-Castellanos et al. 2003). From then, erosive activity and fluvial incision in the Ebro basin has persisted throughout the Quaternary, as shown by the extensive systems of stepped terraces along its rivers (Lewis et al. 2009). The studied paleosol has been developed on the highest and oldest alluvial fan (Qt1) of a well-preserved stepped terrace system of the Alcanadre River. The Qt1 strath terrace is now an encrusted surface (calcretised), 170 m above the present channel (relief inversion) and it has a broad fan shape with a mean slope reaching 1%. It forms the water divide between the Alcanadre and Cinca Rivers. This highest surface is considered to be related to the initial stages of the configuration of the Ebro Basin's Quaternary exorrheic fluvial network (Meléndez et al. 2011). The Qt2 to Qt4 terraces are missing in this study area (**Figure 1**), but are clearly recognised in northernmost sectors (Rodríguez 1986). Paleomagnetic analysis has shown the Matuyama-Brunhes (779 ka) transition to be located between terraces Qt2 and Qt3 whilst terrace Qt1 is tentatively related to the Jaramillo (around 1000 ka) magnetozone (Lewis et al. 2009). The soil parent materials, coming from the External Pyrenees, are successive fine calcareous detrital sediments (above 4.5 m thick) overlying rounded gravels of limestones, sandstones and conglomerates embedded in a sand matrix.


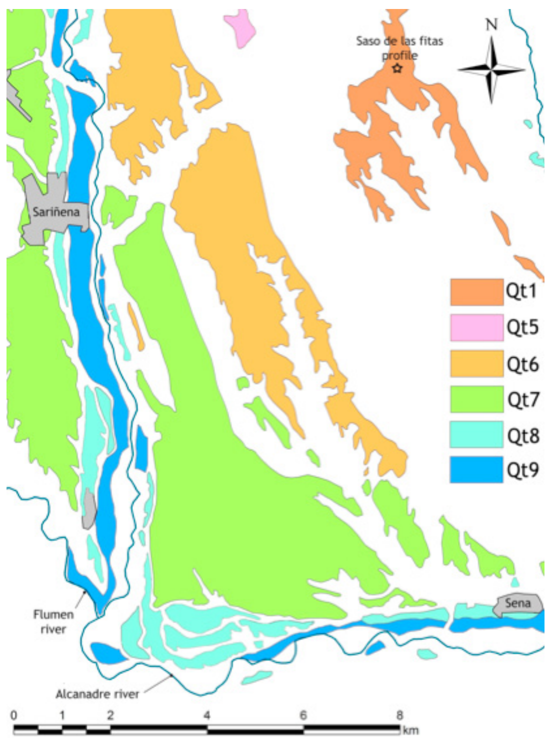


**Figure 1.** Location of the studied profile, developed on the highest and oldest alluvial fan (Qt1) of a stepped terrace system of Alcanadre River (Ebro Basin, NE-Spain).

## 2.2. Soil morphology and sampling

The encrusted surface has allowed the preservation of a great number of horizons below the calcrete (Bkm); in particular the following horizons of the profile were described: Ah-Bkm1-Bkm2-2Bkc-2Btkc-2Btk-3BC-4Ckc-4Ck-5C-6C (**Figure 2**). The soil is classified as Petric Calcisol according to WRB (IUSS 2007) and as Calcic Petrocalcid under a thermic-aridic soil climate regime (Soil Survey Staff 2010).

The paleosol was described in the field according to FAO procedures (FAO 2006), and detailed morphological data were recorded for each horizon. Bulk horizon samples were collected, air-dried, crushed and sieved to 2 mm to remove coarse fragments. These bulk samples were used for physical, chemical and mineralogical characterization. In addition, undisturbed oriented clod samples were carefully extracted to maintain the original structure of the soil, placed in containers and transported to the laboratory for thin section preparation. Peds were also air-dried before being heated to 90 ºC, impregnated under vacuum with epoxy resin, mounted on glass slides and ground to 30 μmm. Thin sections were studied using a petrographic microscope under both plane- and cross-polarized light. The study will be conducted following a systematic approach where types of pedofeatures will be assigned to a given soil formation event following a hierarchy (Fedoroff et al. 2010).

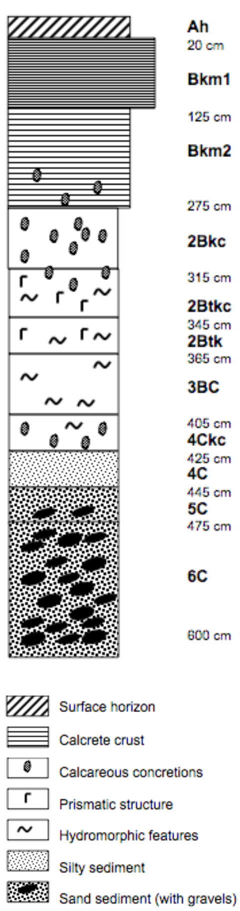


**Figure 2.** Section of the selected profile of Saso (= mesa) de las Fitas showing the arrangement of the different horizons from petrocalcic (at the top) to the gravels (at the bottom) and picture showing the spatial continuity of soil horizons and gravel layers.

### 2.3. Chemical and physical properties analysis

Particle size distribution was determined using the pipette method, after the removal of organic matter using $H_2O_2$ and with Na-hexametaphosphate used as a dispersing agent (Gee and Bauder 1986). Using detailed texture data (USDA subdivisions) from all horizons, all fractions (%) of the fine earth were recalculated removing clay; if one horizon deviated more than 5% from another, a lithological discontinuity was diagnosed.

Soil pH (1:2.5 ratio in $H_2O$) was determined using a glass electrode (McLean 1982). Total carbonate content was measured volumetrically (with a calcimeter) after treatment with 6N hydrochloric acid (Nelson 1982). The electrical conductivity (ECe) and the sodium adsorption ratio (SAR) were measured in the saturated paste extract (Rhoades 1982a). Total soil organic C was determined by the wet oxidation method using the van Bemmelen factor (1.724) to estimate organic matter (Nelson and Sommers 1982). The cation-exchange capacity (CEC) was determined with the $NH_4^+$ ion retention after washing the soil sample with a solution of $NH_4OAc$ 1N at pH 7 (Rhoades 1982b).

### 2.4. Mineralogical characterization

The mineralogical composition of the clay fraction (≤ 2 µm) of selected horizons (Ah, 2Bkc, 2Btk 4Ckc and 5C) was identified by X-ray powder diffraction (XRD) on a Philips X'Pert diffractometer with graphite-monochromated Cu Kα radiation. XRD patterns were obtained from each sample using: a) random powder mounts, and the following oriented aggregates; b) air dried, c) ethylene glycol-solvated, d) heated at 300 ºC and e) 550 ºC for 3 h. Semi-quantitative estimates of quartz, goethite and total phyllosilicates were obtained from the random powder patterns, integrating the area of the maxima diffraction at 0.424, 0.416 and 0.444 nm, respectively, and using the mineral intensity factors reported by Schultz (1964). Approximate abundances of illite, smectite and chlorite were obtained in a similar way, using the oriented aggregate patterns (peak areas at 9.98 nm for illite, 1.65 nm for smectite in ethylene glycol-solvated aggregate and 1.42 nm for chlorite in 550 ºC heated oriented aggregate).

## 3. Results

This section gives the description of the field characteristics, chemical and physical properties, clay mineralogy and the micromorphological features of the paleosol.

### 3.1. Soil morphology

The Ah horizon, up to 20 cm thick, has a brown color in contrast to the underlying horizons: nearly white for Bkm horizons and very pale brown for the rest of horizons with the exception of Bt horizons that become to reddish yellow (**Table 1**). In particular, the petrocalcic horizon consists of 2 subhorizons, a laminar one on the top (Bkm1) and underneath a nodular one (Bkm2), also named pisolithic according to Meléndez et al (2011). The upper petrocalcic subhorizon (Bkm1) is composed of individual laminae (some mm thick) that range in color (dry) from white (N8) to pinkish white (7.5YR 8/2), very pale brown (7.5YR 8/3) and light brown (7.5YR 6/3). In contrast Bkm2 has a very pale brown (10YR 8/3) overall color with white veins, and occasional aggregates with light brown (10YR 6/4) color. The limits between horizons are nearly planar or slightly wavy and clear, with the exception of the petrocalcic horizon that has abrupt limits. The type of structure in Ah horizon is granular, massive in Bkm (petrocalcic) horizons, blocky in Bk (calcic) and prismatic in Bt (argic) horizons, overall with a strong grade or development. Argic horizons have slickensides on the faces of the aggregates. The deepest soil layers (5C, 6C) are structureless and non-coherent because of the sandy texture and stoniness (**Table 1**).

**Table 1.** Main morphological properties of studied horizons

| Horizon | Basal depth (cm) | Colour (dry) | Colour (wet) | Structure (grade, type) | Dry consistence | Mn spots (% v/v)* | Others |
|---|---|---|---|---|---|---|---|
| **Ah** | 20 | 7.5YR 5/4 | 7.5 YR 4/4 | s, G | SO | - | - |
| **Bkm1** | 125 | N 8 to 7.5YR 6/3 | N 8 to 7.5YR 6/4 | ms | EHA | - | cemented |
| **Bkm2** | 275 | N 8 to 10YR 8/3 | N 8 to 10YR 8/4 | ms | EHA | - | cemented |
| **2Bkc** | 315 | 10YR 8/4 | 10YR 6/6 | s, Sbk | HA | - | concretions |
| **2Btkc** | 345 | 7.5YR 7/4 | 7.5YR 5/6 | m, ABk | HA | 10 | slickenside |
| **2Btk** | 365 | 7.5YR 7/6 | 7.5YR 5/8 | m, P | HA | 40 | slickenside |
| **3BC** | 405 | 10YR 8/4 | 10YR 6/6 | m, Abk | HA | 8 | - |
| **4Ckc** | 425 | 10YR 8/4 | 10YR 6/6 | w, Sbk | HA | 5 | concretions |
| **4Ck** | 445 | 10YR 8/4 | 10YR 6/6 | ms | HA | - | - |
| **5C** | 475 | 10YR 7/4 | 10YR 6/4 | ms | HA | - | - |
| **6C** | 600 | Heteroge-neous | Heteroge-neous | sg | LO | - | - |

Structure grade: w, weak; m, medium; s, strong. Structure type: G, granular; Sbk, Subangular blocky; Abk, angular blocky; P, prismatic; sg, single grain; ms, massive. Dry consistence: LO, loose or non-coherent; SO, soft; HA, hard; EHA, extremely hard.

### 3.2. Chemical and physical properties

The soil pH is basic in all horizons, increasing with depth up to 9.0 in bottom horizons. The soil profile is highly calcareous throughout with a maximum in petrocalcic horizons where is higher than 80% w/w. The electrical conductivity (ECe) and sodium adsorption rate (SAR) are very low on the topsoil reaching a maximum at 4 m depth (ECe=17 dS/m; SAR=8 $(mmol/L)^{0.5}$). Organic matter content is negligible below the Ah horizon.

The coarse element content is very low and they have a different lithology: reworked calcrete clasts in the Ah-horizon, hard concretions in different Bkc and Ckc horizons and only gravels in bottom C-layers, the content of which increases with depth (Table 2). Pebble and cobble-sized rounded gravels with intercalated sand lenses are only found at the bottom of the profile (below 5-m depth) and the upper sediments are mainly silt and clay particles, which suggests a progressive reduction of the sediment transport capacity. The abrupt changes in the stoniness, in the sand and silt fractions, and in the clay mineralogy allowed us to define at least 6 periods of parent material deposition (lithological discontinuities).

**Table 2.** Some chemical and physical properties of the paleosol

| Horizon | Depth (cm) | pH $H_2O$ (1:2.5) | Equivalent $CaCO_3$ (%) | ECe (dS/m) | SAR $(mmol/L)^{0.5}$ | OM (w/w, %) | CEC ($cmol_+$/kg) | Stones (v/v, %) |
|---|---|---|---|---|---|---|---|---|
| **Ah** | 20 | 8.1 | 9.4 | 0.7 | 0.2 | 4.4 | 19.4 | 30* |
| **Bkm1** | 125 | - | 87.7 | - | - | - | - | - |
| **Bkm2** | 275 | - | 83.7 | - | - | - | - | - |
| **2Bkc** | 315 | 8.2 | 48.8 | 3.1 | 1.6 | 0.3 | 8.2 | 20** |
| **2Btkc** | 345 | 8.3 | 40.8 | 7.9 | 3.7 | 0.2 | 17.7 | 10** |
| **2Btk** | 365 | 8.2 | 39.5 | 14.2 | 6.1 | 0.2 | 11.9 | negligible |
| **3BC** | 405 | 8.1 | 46.1 | 17.1 | 8.0 | 0.2 | 8.6 | negligible |
| **4Ckc** | 425 | 8.2 | 46.5 | 15.5 | 5.6 | 0.2 | 8.8 | 10** |
| **4Ck** | 445 | 8.4 | 47.0 | 8.7 | 3.9 | 0.2 | 3.9 | negligible |
| **5C** | 475 | 9.0 | 38.8 | 0.8 | 1.8 | <0.2 | 3.5 | 5*** |
| **6C** | 600 | 9.0 | 11.7 | 0.4 | 0.9 | <0.2 | 1.2 | 50*** |

* fragments of calcrete; ** concretions: ***gravels

The textural class is loam in the Ah horizon, silt loam in 2Bkc, 3BC, 4Ckc, 4Ck horizons, silty clay loam in the 2Btkc and 2Btk horizons, and it becomes sandy in the deepest C-layers (Table 3).

**Table 3.** Particle size analyses of the paleosol

| Horizon | Textural Class USDA | VCS 2-1 mm (%) | CS 1-0.5 mm (%) | MS 0.5-0.25 mm (%) | FS 0.2-0.1 mm (%) | VFS 0.1-0.05 mm (%) | CSilt 0.05-0.02 mm (%) | FSilt 0.02-0.002 mm (%) | Clay <0.002 mm (%) |
|---|---|---|---|---|---|---|---|---|---|
| **Ah** | Loam | 3.0 | 3.1 | 5.5 | 9.7 | 19.3 | 11.5 | 27.1 | 20.8 |
| **2Bkc** | Silt Loam | 2.9 | 2.2 | 1.7 | 2.4 | 4.6 | 16.0 | 46.3 | 23.9 |
| **2Btkc** | Silty Clay Loam | 0.6 | 1.1 | 1.2 | 3.4 | 4.1 | 11.1 | 50.6 | 28.0 |
| **2Btk** | Silty Clay Loam | 0.1 | 0.2 | 0.4 | 1.9 | 3.1 | 9.4 | 53.5 | 31.5 |
| **3BC** | Silt Loam | 0.1 | 0.2 | 0.4 | 7.2 | 15.6 | 18.8 | 37.8 | 20.0 |
| **4Ckc** | Silt Loam | 1.7 | 1.2 | 1.8 | 5.6 | 5.5 | 11.0 | 47.5 | 25.7 |
| **4Ck** | Silt Loam | 0.2 | 0.6 | 1.8 | 10.6 | 8.8 | 14.2 | 41.6 | 22.2 |
| **5C** | Sandy Loam | 1.5 | 4.4 | 18.3 | 26.8 | 14.4 | 12.8 | 12.7 | 9.1 |
| **6C** | Sand | 3.6 | 17.7 | 43 | 26.1 | 1.6 | 3.1 | 2.1 | 2.9 |

Abbreviations: VC, Very Coarse; C, Coarse; M, Medium; F, Fine; VF, Very Fine; S, Sand.

### 3.3. Mineralogical characterization

The semi-quantitative mineralogical composition (Table 4) indicated that dioctahedral mica (illite) is by far the most abundant phyllosilicate (ranging from 40 to 70%) reaching the highest content in the upper horizon Ah). Smectite and chlorite are present in many horizons in small proportions (for both cases not more than 12%). Goethite has also been detected in some horizons but in a very small proportion (traces, ≤ 2%), although enough to redden the horizons. The mineralogical composition of the 2Bkc and 2Btk horizons was very similar, but not the rest of horizons. This confirms the presence of the above-mentioned discontinuities corresponding to different sedimentary processes (Table 4). XRD results of the ≤ 2 µm fraction of selected horizons showed the absence of fibrous minerals (palygorskite and sepiolite) in all samples. The XRD patterns of the 2Bkc horizon are shown as an example (Figure 3).

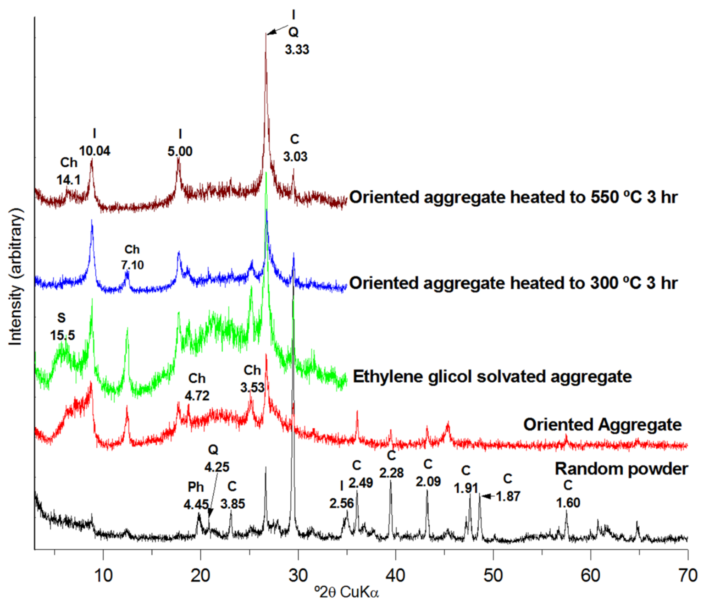


**Figure 3.** XRD patterns of the ≤ 2 µm fraction of the 2Bkc horizon. Numbers indicate *d*-values (x $10^{-1}$ nm). S, smectite; Ch, chorite; I, illite; Q, quartz; Ph, phyllosilicates; C, calcite.

**Table 4.** Semi-quantitative (relative %) mineralogical composition of the clay fraction of selected horizons of the paleosol

| Horizon | Thickness (cm) | Calcite | Quartz | Illite | Smectite | Chlorite | Kaolinite | Goethite |
|---|---|---|---|---|---|---|---|---|
| **Ah** | 0-20 | 11 | 11 | 70 | 0 | 8 | 0 | tr |
| **2Bkc** | 275-315 | 35 | 7 | 43 | 7 | 8 | 0 | 0 |
| **2Btk** | 345-365 | 35 | 6 | 42 | 8 | 9 | 0 | tr |
| **4Ckc** | 405-425 | 26 | 10 | 44 | 12 | 0 | 8 | tr |
| **5C** | 475-495 | 35 | 15 | 42 | 3 | 5 | 0 | 0 |

0, not detected; tr, traces (≤ 2%).

Illite is the most common mineral component of the clay fraction in soils of the region (Badía et al. 2009b). Illite and chlorite phyllosilicates are considered to be inherited from the parent material. Smectites could be either inherited or result from the transformation of illite in an environment with poor drainage, high pH and abundance of basic cations (Wilson 1999).

### 3.4. Micromorphology

Some common trends can be found in all horizons, such as the absence of organic components below the Ah horizon and the crystallitic b-fabric due to the presence of micrite and microsparite (Table 5). Calcite accumulations, textural pedofeatures, and manganese coatings are frequent along the profile (Table 6).

**Table 5.** Main micromorphological properties of the groundmass of the studied horizons

| Horizon | Basal depth (cm) | Pedality | Void | C/F ratio and related distribution (limit 20 µm) | Coarse elements | Micromass | b-fabric |
|---|---|---|---|---|---|---|---|
| **Ah** | 20 | | | | | | |
| **Bkm1** | 125 | Massive laminar cemented | 10%, compound packing pores | - | - | Micrite & microsparite | crystallitic |
| **Bkm2** | 275 | Massive laminar and nodular cemented | 10%, compound packing pores | - | - | Micrite & microsparite | crystallitic |
| **2Bkc** | 315 | Moderate subangular blocky | 15%, channels, vughs and chambers | 1/1 close porphyric | Fresh angular quartz and fresh sparite | Micrite & microsparite | crystallitic |
| **2Btkc** | 345 | Moderate prismatic and channels | 15%, planar vertical, channels, vughs and chambers | 3/1 single-space porphyric | Fresh angular quartz and fresh sparite | Micrite & microsparite | crystallitic |
| **2Btk** | 365 | Moderate prismatic | 20%, planar vertical, channels, and vughs | 1/1 double- space porphyric | Fresh angular quartz | Micrite & microsparite | crystallitic |
| **3BC** | 405 | Moderate prismatic | 10%, planar vertical, vesicles and channels | 1/1 double space porphyric | Fresh angular quartz | Micrite & microsparite | crystallitic |
| **4Ckc** | 425 | Weak prismatic to subangular blocky | 25%, planar, channels, and vughs | 1/1 double-space porphyric | Fresh angular quartz | Microsparite & micrite | crystallitic |
| **4Ck** | 445 | Apedal | 10% channels, and vughs | 1/1 double-space porphyric | Fresh angular quartz | Microsparite & micrite | crystallitic |
| **5C** | 475 | Apedal | 20% vughs and vesicles | 3/1 close porphyric | Fresh angular quartz | Microsparite & micrite | crystallitic |

**Table 6.** Micromorphological pedofeatures of the studied horizons

| Horizon | Basal depth (cm) | Pedofeatures |
|---|---|---|
| **Ah** | 20 | Not performed. |
| **Bkm1** | 125 | Cemented horizon, with a massive-laminar structure. It includes embedded spherical peds in a gently undulating band matrix of micrite and sparite that sometimes form pendants. |
| **Bkm2** | 275 | Cemented horizon, nodular and banded. It is composed of alternating bands of orthic micrite nodules packed between relatively pure micritic laminar bands and occasional sparite intercalations. |
| **2Bkc** | 315 | Coatings and infillings of microcrystalline calcite in old channels and orthic nodules and soft concretions (some geodic), which indicate an in situ accumulation process. Scarce hypo- and quasi-coatings of manganese oxides around pore channels and cracks. Some decarbonated zones. |
| **2Btkc** | 345 | Microlaminated pockets of clay intercalations fragmented by vertical cracks or distorted by nodules of micrite. Decarbonated zones associated with sorted intercalations. Coarse orthic nodules of dense micrite superimposed on textural pedofeatures. Hypo- and quasi-coatings of manganese oxides around pore channels and cracks. |
| **2Btk** | 365 | Interbedded microlaminated clay pockets, not associated with current or past pores Impregnative nodules of micrite, rounded and lobulated, filling old channels. Hypo-coatings of manganese and dendritic aggregate nodules of manganese and iron oxides. |
| **3BC** | 405 | Microlaminated clay and silt as coatings on channel walls. Sorted wavy intercalations, with a subhorizontal orientation. Dendritic aggregate nodules of manganese within the peds and hypo- and quasi-coatings of manganese oxides around pore channels. |
| **4Ckc** | 425 | Orthic nodules of calcite, impregnative and diffuse. Sand size nodules of manganese and iron oxides around channels. Scarce intercalations of microlaminated clay and silt (dusty clay) weakly oriented. |
| **4Ck** | 445 | Dendritic nodules (0.1 to 0.2 mm) of manganese around pore channels. |
| **5C** | 475 | Coatings of microlaminated clay and silt (dusty clay) in some macropores. |
| **6C** | 600 | Not performed. |

Petrocalcic horizons (stage V, Machette 1985) have an average thickness of 255 cm and they were divided into two subhorizons in the field based on their hardness and their morphology. The Bkm1 horizon (about 1-m thick) is extremely hard and dense (2.3-2.4 g/cm$^3$) because $CaCO_3$ plugs the horizon, with the highest carbonate content (ca 88% w/w) of the profile, and a massive-laminar structure (**Figure 4A**). Under the microscope, the laminar petrocalcic horizon consists of an alternation of gently undulating bands of micrite and sparite that sometimes form layered pendants, also known as vadose microstalactitic calcite cements (**Figure 4B**). Pendant laminae are mostly vertical, consistent with the direction of gravity. The pendants show an internal lamination, lighter than the outer coating. These morphologies are commonly recognized in petrocalcic laminar horizons of the zone (Meléndez et al 2011). Although no EDAX analyses have been performed, the layering seems to correspond to different crystal size owing to different precipitation conditions. Within the laminar petrocalcic horizon there are variety of features such as spherical peds (**Figure 4C**). These peds comprise a thin coating of clay-sized material around a core, which includes pores and mineral grains sometimes with laminar structure. These are not considered to be ooids or pisoliths, since these peds are more clayey that the surrounding carbonate matrix, and are not formed as concretions (precipitation around a nucleus), but by some type of argilloturbation (internal granostriation).

The Bkm2 horizon (150 cm thick) is more porous (2.0 g/cm$^3$) and has a slightly lower carbonate content (ca 84% w/w) than the overlying laminar Bkm1 horizon; it shows a massive appearance with nodular structures inside (**Figure 4D**). The Bkm2 horizon has a spaced framework of orthic micrite nodules packed between relatively pure micritic laminar layers (**Figure 4E**). This type of nodule, orthic and without a concentric internal fabric, suggests a progressive enrichment of calcium carbonate in fairly constant conditions. Underlying those petrocalcic horizons is a calcic horizon (2Bkc). Different calcite accumulation types appear in the 2Bkc horizon such as coatings, infillings and orthic nodules, which indicate an in situ calcite accumulation process. The connectivity of rounded gravel sized nodules of calcite suggests that they were formed around roots (and thus are also named rhizoconcretions or rhizoliths, **Figures 5A** and **5B**). Under this nodular calcic horizon, two subhorizons (2Btkc and 2Btk) show evidence of strong clay enrichment. Both have about 30% of clay particles (1.25 times higher than the upper horizon), a reddish colour, goethite traces and an angular blocky (**Figure 5A**) or prismatic structure (**Figure 5C**), defining characteristics of an argic horizon (argillic by STS). Argic horizons are recarbonated, as shown by the presence of micrite accumulations in nodular forms (**Figure 5B**), especially in the upper subhorizon (2Btkc). The presence of smectites and chlorites (both around 8%) could account for the strong prismatic structure, soil cracking and some argilloturbation. A common feature in the argic horizons, and also the underlying horizons (from 315 to 425 cm depth), is the presence of Fe/Mn accumulations (**Figures 5D, E**) that, in the field, have been described with percentages varying from about 5% to 40% by volume. Micromorphologically, two types of Fe/Mn accumulations (gleyed horizons) were distinguished: (1) hypo- and quasi-coatings related to pore channels, and (2) dendritic aggregate nodules within the peds (**Figure 5D**). These morphologies indicate moderate to strong redox conditions. Two kinds of textural pedofeatures can be distinguished in the argic horizons: (1) interbedded microlaminated clay pockets (**Figure 5F**), sometimes fragmented and distorted by micrite accumulations and (2) few fine clay coatings along vertical cracks and around calcite channel infillings.

A new calcic horizon appears at the bottom of the profile (4Ckc), again with rhizoconcretions but in this case not as rounded (**Figure 6A**) as in the upper nodular calcic horizon (2Bkc) and the recarbonated argic horizon (2Btkc). Moreover, coatings of microlaminated clay and silt (dusty clay) can be found until 4.5 m soil depth in some macropores. These dusty clay coatings appear covered by micrite (**Figure 6B**), which demonstrates the recarbonatation process occurred after clay illuviation.

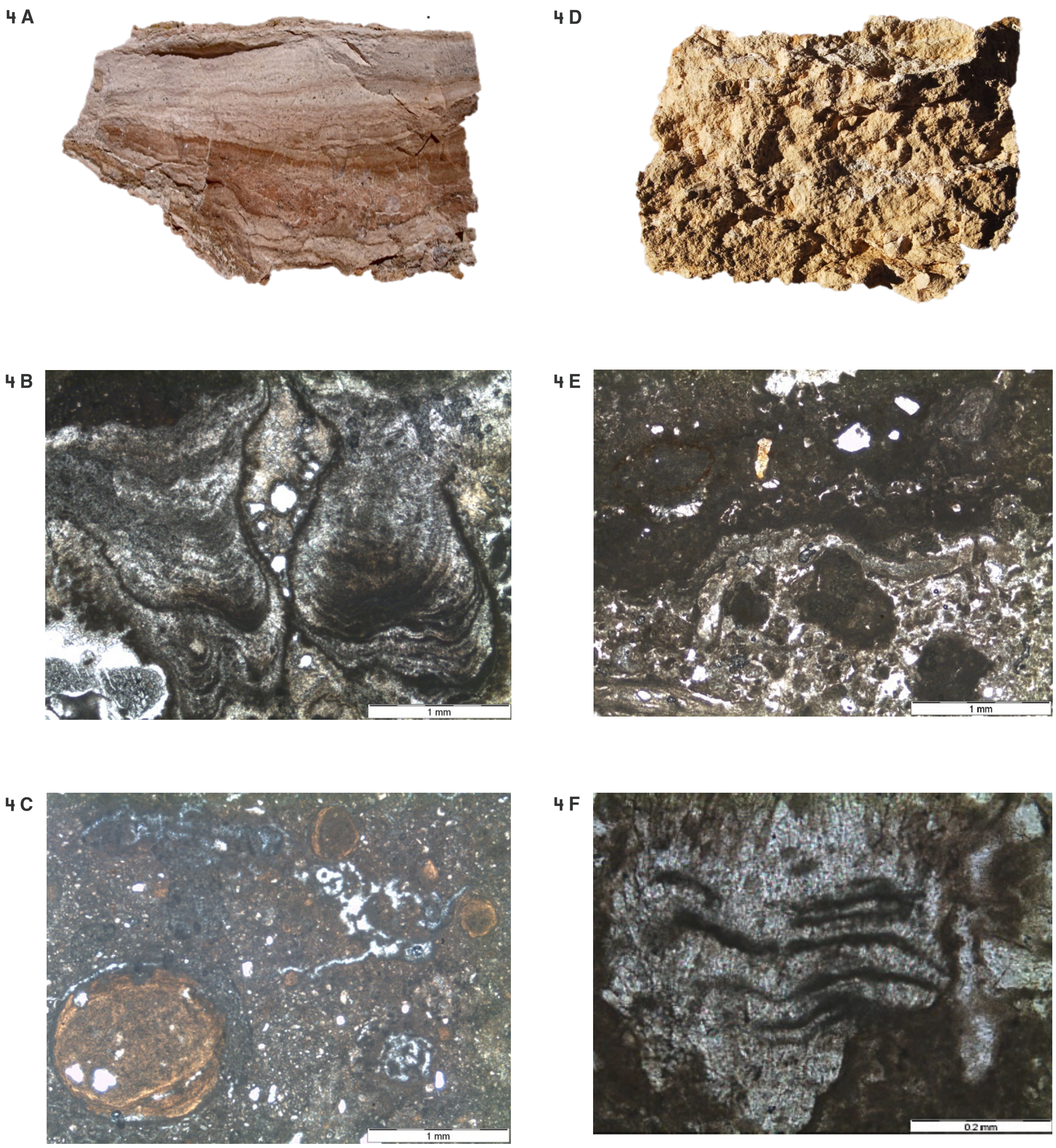


**Figure 4.** Pedofeatures in the upper part of the paleosol. **A**: Section of upper petrocalcic horizon (Bkm1) showing small-scale wavy layers (laminar one or bacon steak like). **B**: Photomicrograph of the alternation of micrite layers and vadose microstalactitic sparite cement in Bkm1 horizon. **C**: Photomicrograph of spherical peds in the laminar petrocalcic horizon (Bkm1). **D**: Section of lower petrocalcic horizon (Bkm2), nodular type. **E**: Spaced framework of orthic micrite nodules packed between relatively pure micritic layers in Bkm2 horizon. **F**: micritic laminar bands within sparite intercalations in Bkm2 horizon. All photomicrographs (**B, C, E, F**) in plane-polarized light.

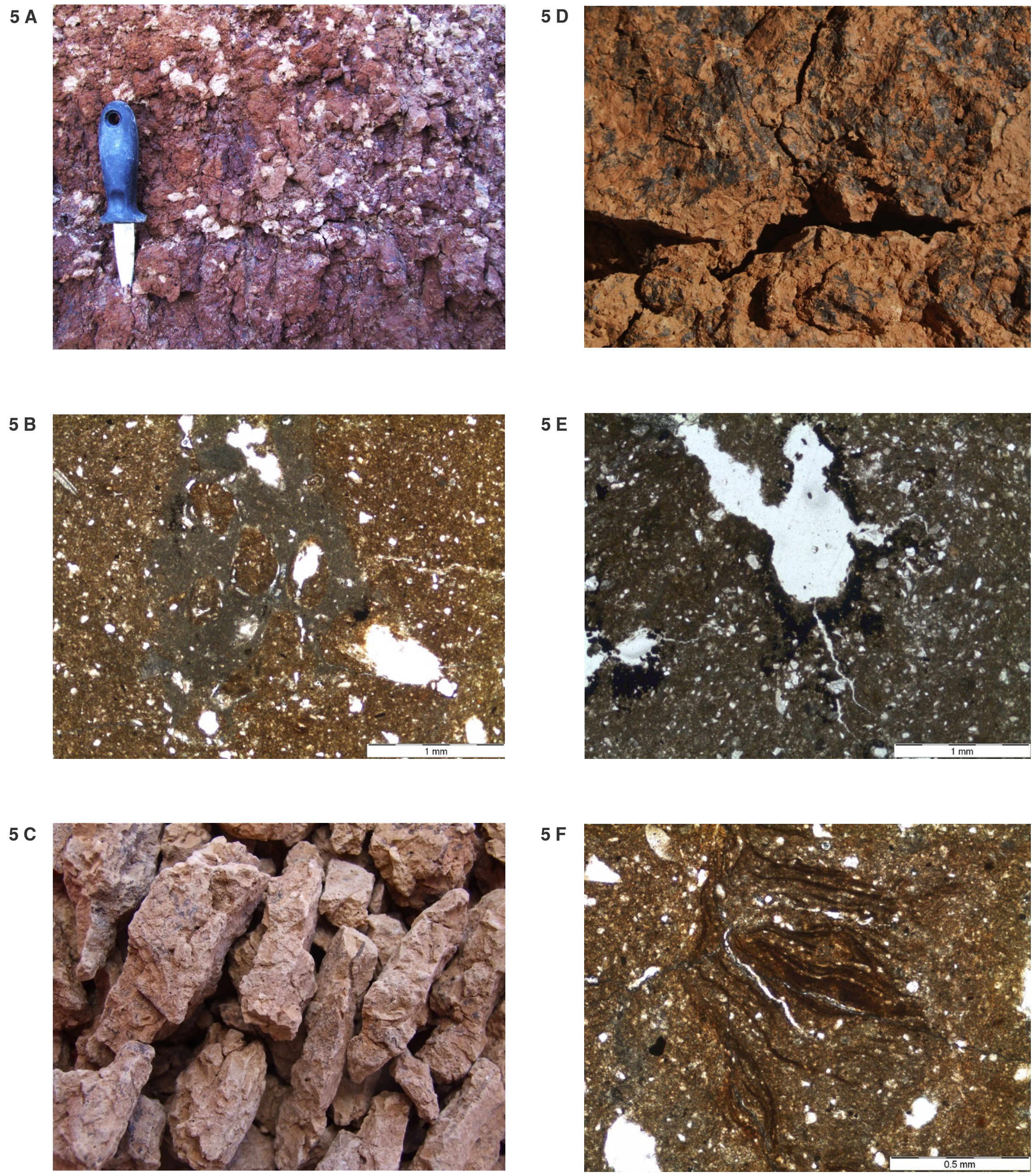


**Figure 5.** Pedofeatures in the recarbonated argic horizons (2Btkc and 2Btk) of the paleosol. **A**: Rounded carbonate nodules in 2Btkc horizon (345-365 cm) in transition to reddish and prismatic peds of 2Btk horizon (365-405 cm). **B**: Photomicrograph of a rizholith-like nodule of impregnative micritic calcite superimposed in a clay-rich area in 2Btk. **C**: Prisms of the 2Btk horizon, with coatings of manganese oxides in ped faces. **D**: Detail of manganese oxides coatings (black spots) and clay coatings (bright surfaces) in cracked prisms faces (2Btk). **E**: Photomicrograph of hypo-coatings of manganese oxides around pore channels. **F**: Interbedded microlaminated clay pockets in 2Btk horizon. All photomicrographs (**B, E, F**) in plane-polarized light.

6 A

6 B

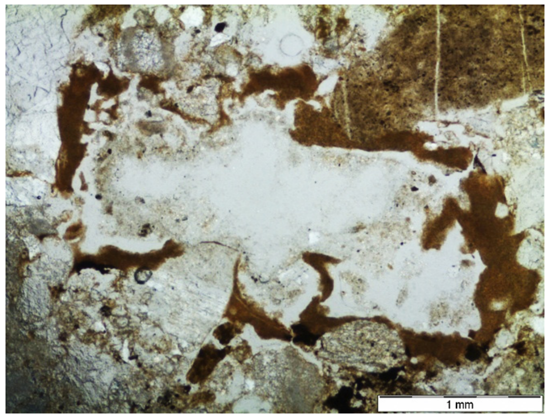


**Figure 6.** Pedofeatures in the lower part of the profile. **A**: Irregular carbonate rhizoconcretions in 4Ckc horizon. **B**: Photomicrograph in plane-polarized light showing a macropore coated of microlaminated clay and silt (dusty clay) covered by micritic calcite (5C horizon).

# 4. Discussion

## 4.1. Pedofeatures in the paleosol

Laminar crusts have been interpreted as the latter stage of cementation with or without the influence of biological activity (Durand et al. 2010). Petrocalcic horizons with nodules of micrite are frequently overlain by laminar horizons (Meléndez et al. 2011). Moreover, in this case, the petrocalcic nodular horizon is underneath a nodular calcic horizon. The morphology of the nodules (orthic and without internal fabric) and their arrangement in columns suggest that they were formed around roots (rhizoconcretions or rhizoliths) in fairly constant conditions. In any case these conditions of pedogenesis would alternate with erosion and sedimentation events (Meléndez et al. 2011). The presence of spherical peds within the laminar petrocalcic horizon could be evidence of that succession of processes; their formation according to Alonso-Zarza and Jones (2007) requires an initial fragmentation of the groundmass and a posterior coating formation by the biogenic activity of roots and associated microorganisms. Their origin is also interpreted to be old excrements of earthworms or molluscs, which were later cemented by calcite (Kooistra and Pulleman, 2010).

Below the petrocalcic and calcic horizons a thick argic horizon (with two subhorizons: 2Btkc and 2Btk) has been described, according to the macroscopic or microscopic characteristics. At present this horizon has a high carbonate content, both in the fine earth fraction and in the clay fraction (Tables 2 and 4). Because polyvalent cations cause flocculation, the argic horizon must have formed after decarbonation and therefore it is most likely to be a paleofeature related to a wetter climate than present (Khormali et al. 2003; Quénard et al. 2011). Environmental changes with new contributions of calcareous sediments allowed the extensive carbonation of this argic horizon, which now has a crystallitic b-fabric. Environmental changes provided further sediments, which indicate that the supposedly abandoned terrace continue to be active even though the fluvial network was entrenched (Meléndez et al. 2011). A scarce plant cover, with steppe landscapes and open *Pinus* woodlands at least during the cold spells of the Late Pleistocene in this continental region (González-Sampériz et al. 2010), ensured sediment aggradation. The recarbonation hypothesis is supported by (1) the existence of sorted decarbonated zones that still keep the original sediment structure, and (2) the fact that nodules appear as dense micritic impregnations superimposed on the textural pedofeatures. Calcite depletion can be also noticed in the 2Btkc and 2Btk horizons, as subhorizontal areas not associated with current or past pores. They can be better interpreted as original, non-recarbonated zones formed as the result of a more recent decarbonation process.

Similarly, sparite and recarbonated argillans were found in the oldest terrace (Early Pleistocene) of the Segre River (Badía et al. 2009a) that were interpreted as pedological paleofeatures caused by climate changes during the Quaternary. Analogously, Khormali et al. (2003) found clay coatings superimposed on carbonate coatings in argic horizons of calcareous soils. The clay coatings, in turn, were covered by calcite, indicating recalcification. They considered that argic horizons were formed in a previous less arid climate than the current semiarid regions of southern Iran (with a MAP about 340 mm/yr and a P/ETo ratio between 0.3-0.5).

In the field, shiny surfaces considered to be clay skins were seen in the recarbonated argic horizons (**Table 5**). However, in thin sections, microlaminated clay coatings rarely can be found. The main factor responsible for the absence of clay coatings in old argic horizons is their physical disturbance by shrinking and swelling in soils with high clay contents and periodic moist and dry phases (Khormali et al. 2003; Mermut and Pape 1971). Instead, intercalative microfacies are abundant in the recarbonated argic horizons. Intercalative microfacies formation can be related to soil formation process in sodic soils (Rodríguez et al. 1990; Badía et al. 2011), the possibility of which must be discarded in this soil environment, or to waterlogging events (Fedoroff and Courty 2012), and is more likely in this situation. According to these authors, water with high energy percolates through the surface horizon along macropores, which produces a turbulent flow and therefore a micro-erosion or degradation at the top of the argic horizon, especially if this horizon is shallower (ie by previous exhumation). This energy decreases with depth, leading to progressive settling of microlaminated pockets, especially in old cracks related to the swelling activity of the smectites during dry/dessication periods. Moreover although carbonate may prevent the dispersion of clay, the movement of already dispersed clay (and silt) can take place if pores are large enough (Pazos 1990). Another interpretation that may explain the presence of intercalative microfacies is related to the decrease of redox potential in wet conditions that transforms the ferric iron into ferrous iron that was removed in pseudo-soluble forms. Destruction of the ferric bindings leads to a structural collapse resulting in a loose packing of soil constituents. The partial ferric ion removal would favour mass internal displacement. In calcareous environments, however, this process would be more seldom. Reducing conditions had to be in the soil at some time that resulted in a $Fe^{2+}$ and $Mn^{2+}$ ion increase; these conditions could coincide with a decrease in soil reaction and calcite depletion, allowing clay illuviation. Afterwards, the pedoclimate changed to oxidized, with warmer and drier conditions that oxidated $Fe^{2+}$ ions via solution to form goethite that gives the horizons their reddish yellow colour. With new well-aerated conditions, also Mn solubility decreases and Mn coatings and nodules can be formed. Moreover, Mn solubility decreases with an increase in soil pH by a factor of 10 for each pH unit. This increase in pH would be given by aggradation of calcareous sediments above soil or new inputs of calcite saturated water solution, as we mentioned earlier (Ortiz et al. 2002; Lequy et al. 2012).

### 4.2. Environmental conditions and time for paleosol formation

The carbonate enrichment in the subsoil resulting in nodular calcic horizons or petrocalcic horizons represents again an unequivocal indicator for autochthonous soil formation (Zielhofer et al. 2009). The large thickness of both overlaid petrocalcic horizons, its high carbonates content (> 80%), and its strong degree of induration could express hundreds-of-thousands to millions of years of development in arid environments (Machette 1985; Brock and Buck 2009; Monger et al. 2009). Because the depth of the calcic horizons is correlated with the depth of water penetration (Dan et al. 1981; Sheldon and Tabor 2009), the relatively shallow formation of Bkm horizons could indicate that the climate was progressively drier. Some authors (Birkeland 1999; Dan et al. 1981) consider that the presence of calcrete infers a paleoprecipitation below 500 mm $yr^{-1}$.

But if the unique source of calcium carbonated accumulated in current thick subsurface horizons is the leaching from topsoil horizons, the current Ah horizon (20 cm thick) cannot explain the intense carbonate accumulation. Erosion of former upper horizons as well as inputs of allochthonous carbonates in the alluvial fan, through dust inputs (Lequy et al. 2012) or the subsurface flow (Ortiz et al. 2002; Poch et al. 2012), should be also considered. In the studied paleosol, the occurrence of vertical layered pendants or vadose microstalactitic calcite cements reveals a vertical and slow water flow more than an oblique flow (**Figure 4B**).

Beside carbonation, clay illuviation is another common pedofeature in semiarid to subhumid regions in relatively stable landforms (Dan et al. 1981; Dorronsoro and Alonso 1994; Roquero et al. 1999; Gallardo et al. 2002; Ortiz et al. 2002; Khormali et al. 2003). Hamer et al. (2007) considered that argic horizon formation (Luvisol-like pedotype) was dominant within the Late Oligocene-Early Miocene in the Ebro Basin; they estimated that an argic horizon (Bt) occurred over 10 ka with a MAT about 10-14 ºC (± 4 ºC) and a MAP of 560-830 mm $yr^{-1}$ (± 200 mm $yr^{1}$). Similarly, Quénard et al. (2011) estimated that the complete decarbonation and desaturation (prior to argilluviation or lessivage) of loess (with 20% carbonate content) needs over 13.6 ka for an annual effective rainfall (rainfall-evapotranspiration) about 150 mm. After that, the lessivage takes place during a similar period to form an argic horizon (Finke and Hutson 2008). Also in alluvial sequences of the mid-Medjerda floodplain (Northern Tunisia), Zielhofer et al. (2009) found argic horizons with many distinct clay films on ped faces above nodular calcic horizons on Late Pleistocene surfaces (Calcic Luvisols, Chromic); they estimated that between 10 and 40 ka are required to develop this pedotype. Intense processes of clay illuviation, rubification and carbonation, successively superimposed, has been found in Early Pleistocene surfaces in Spain (Roquero et al. 1999; Gallardo et al. 2002; Ortiz et al. 2002). Some Petric Cutanic Luvisols (Petrocalcic Palexeralfs by STS) can be still found in some preserved Early Pleistocene glacis of Somontano, in the north of the Monegros Desert and with a wetter current pedoclimate (Badía et al. 2009b).

Dan et al. (1981) observed a good correlation between present-day mean long-term rainfall, related to the depth of moisture penetration into the soil, and the presence of salic, gypsic, calcic and argic horizons in Israel. They found Chromic Luvisols in humid environments (MAP about 500-650 mm $yr^{-1}$), Calcic Luvisols or Luvic Calcisols in semiarid regions (350-500 mm $yr^{-1}$) and Petric Calcisol in driest areas with vegetation changing from Mediterranean sclerophyllous wood to open scrublands. Some equations have been proposed to relate Bk thickness and MAP (Retallack 2005); according to this work, a calcic horizon 40 cm thick, as in this study, gives a MAP estimation of 374 mm $yr^{-1}$.

It is deduced that soils converge towards very specific pedofeatures, and therefore pedotypes (**Table 7**), which depend on the duration of pedogenic processes, geomorphological stability, and climate changes during the Pleistocene in Mediterranean areas (Gónzalez-Sampériz 2004; Markovic et al. 2011; Moreno et al. 2012). The described paleosol, with a Calcic Luvisol-like pedotype buried by a Petric Calcisol-like pedotype, suggests that, despite climatic periodic oscillations, the initially moderately humid climate tends to a progressively drier one.

### 4.3. Model of soil evolution

The pedofeatures and the organization of soil horizons within this paleosol provide information on the Quaternary environmental changes required for its formation, and allow the proposal of a model of polygenetic soil evolution (**Figure 7**). These are still to be dated.

In the first stages of organisation of the exorheic fluvial network of the Ebro Basin (Pliocene), high sedimentation rates deposited coarse gravels and sand without signs of pedogenesis. The sedimentation rate decreased progressively with the accumulation of silt and clay. Later a period of landform stability and humid climate lead to the formation of the argic and nodular calcic horizon sequence (Calcic Luvisol-like pedotype). The presence of paleo-decarbonated zones associated with sorted intercalations and in situ carbonate accumulations support this hypothesis. Increased aridity coupled

**Table 7.** Soils on Pleistocene surfaces in Mediterranean environments: A revisitation of existing data

| Pedotype | Geoform Age | Location | Source |
|---|---|---|---|
| Petric Luvisol (Rhodic) | Early to Middle Pleistocene (stable) | Tajo River terraces (Central Spain) | Roquero et al. (1999) |
| Petric Calcisol | Younger or unstable | | |
| Haplic Calcisol | | | |
| Petric Luvisol | Middle Pleistocene | Almar River terraces (W- Spain) | Dorronsoro and Alonso (1994) |
| Haplic Luvisol | Late Pleistocene | | |
| Ferric Luvisol | Early Pleistocene | Tajo River terraces (Central Spain) | Gallardo et al. (2002) |
| Vertic Luvisol | | | |
| Petric Calcisol | Middle Pleistocene | | |
| Calcic Luvisol | Late Pleistocene | | |
| A-Btk-Ckm | Early Pleistocene | Alluvial fans (Granada Basin, SE- Spain) | Ortiz et al. (2002) |
| (A)-Bt-Ck | Middle Pleistocene | | |
| Petric Calcisol | Older-mid Late Pleistocene to Early Pleistocene | Segre River terraces (Ebro Basin, NE-Spain) | Badía et al. (2009a) |
| Haplic Calcisol | Youngest Late Pleistocene | | |
| Calcic Luvisol (Chromic) | Late Pleistocene | mid-Medjerda floodplain (N-Tunisia) | Zielhofer et al. (2009) |
| Calcic Luvisol (Chromic) | Older Middle Pleistocene | Danube basin Loess (N-Serbia) | Markovic et al. (2011) |
| Chernozem | Late Pleistocene | | |

with a reduction in plant cover and soil erosion caused the truncation of the profile (at least the Ah horizon). New deposition of calcareous sediments caused the recarbonatation of the argic horizon under wetter paleohydrological conditions. A subhumid climate, with waterlogging events, lead to the leaching of calcium carbonate into the argic horizon where, because of its low hydraulic conductivity, hydromorphic pedofeaures (coatings and nodules of Mn and Fe, microlaminated clay pockets displacement) were developed. Smectites could be formed in these ponding conditions, with a high pH and abundance of basic cations. After this subhumid climate and geomorphological stability, the transition to a drier climate developed a new calcic horizon (Haplic Calcisol-like pedotype) with calcite rhizoconcretions. During or after the formation of the upper nodular calcic horizon, a low sedimentation rate and/or increased aridity shifted the carbonate precipitation to shallower depths. Continued carbonate accumulation eventually cemented the horizon to form the petrocalcic one (Petric Calcisol-like pedotype). At least two petrocalcic horizons can be described: at the top, a massive-laminar one, with layers of micrite and sparite that sometimes form pendants, and an underlying nodular one, where orthic micrite nodules are packed between relatively pure micritic laminar layers. The thickness of both overlying petrocalcic horizons, their high carbonate content and their high degree of induration means that a significant amount of time was required to form them under semiarid conditions. The current shallow formation of Bkm horizons may indicate an increase of aridity and/or a new erosional event that removed the upper Ah horizon and incorporated fragments of Bkm horizon.

In summary, the presence of calcic horizons under and over an argic horizon proves the existence of environmental changes throughout the Pleistocene. Despite these fluctuations, the pedogenesis for last hundreds of thousands of years in the Ebro Basin, like other semiarid Mediterranean regions, converges towards the formation of argic, calcic or petrocalcic horizons. The succession of Luvisol pedotypes and pedofeatures towards a Petric Calcisol shows an increasing dryness during the Pleistocene in the semiarid Ebro Valley.

## 5. Acknowledgements

This project was supported by the Instituto de Estudios Altoaragoneses (Diputación de Huesca). The suggestions of editors and anonymous reviewers have greatly improved the original manuscript. Also, we thank José Antonio Cuchí who guided us in the first profile visits and stressed the importance of its study many years ago.

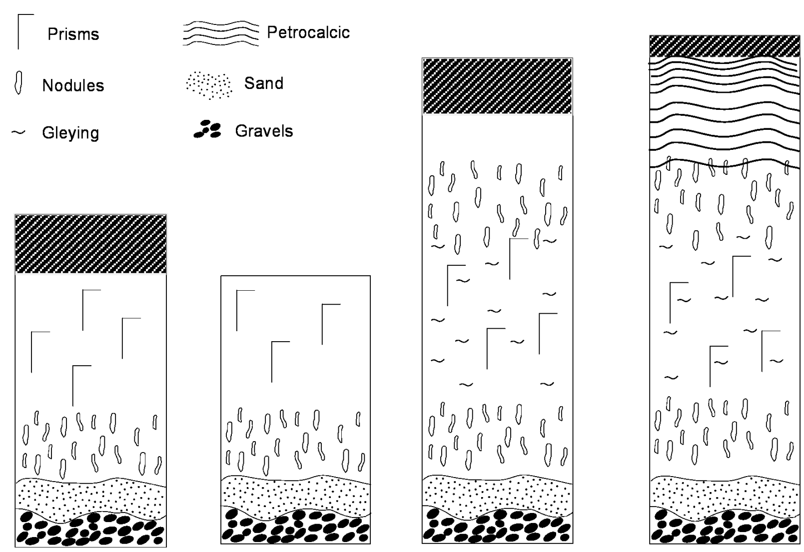


| | | | | |
|---|---|---|---|---|
| Pedotype-like | Calcic Luvisol → | A-horizon truncation → | Haplic Calcisol → | Petric Calcisol |
| Processes | Argilluviation Calcification | Erosion | Cumulization Gleying Calcification | (Petro-) Calcification |
| Pedafeatures | Textural pedofeatures Decarbonated zones Calcite nodules | Micro-erosion: clay pockets displacement, dusty clay illuviation | Coatings and nodules of Mn/Fe Clay pockets Coatings, infillings and nodules of calcite | Laminar bands, pendants and nodules of calcite Cementation |
| Climate | Humid (500-650 mm $yr^{-1}$) | Semiarid (< 350 mm $yr^{-1}$) | Waterloggging events Subhumid (350-500 mm $yr^{-1}$) | Gradual increase in aridity |

**Figure 7.** Proposed evolution model for the Saso de las Fitas paleosol with main soil processes and features.

## REFERENCES


• Alonso-Zarza AM, Jones BJ. 2007. Root calcrete formation on Quaternay karstic surfaces of Grand Cayman. Geologica Acta 5:77-88.

• Badía D, Cuchí JA, Ibarra P, Longares LA, Macías F, Martí C, Peña JL, Pérez C, Poch RM, Romero D, Sancho C, Saz MA, Silva J. 2009b. Itinerarios edáficos por el Alto Aragón. Colección de Estudios Altoaragoneses, nº 28 Huesca: Ed. Instituto de Estudios Altoaragoneses. 190 p.

• Badía D, Martí C, Palacio E, Sancho C, Poch RM. 2009a. Soil evolution over the Quaternary period in a semiarid climate (Segre river terraces, northeast Spain). Catena 77:165-174.

• Badía D, Martí C, Poch RM. 2011. A soil toposequence characterization in the irrigable land-protected area contact zone of El Basal, NE-Spain. Arid Land Research and Management 25:1-18.

• Birkeland PW. 1999. Soil and geomorphology. 3rd edition. New York: Oxford University Press. 430 p.

• Brock AL, Buck BJ. 2009. Polygenetic development of the Mormon Mesa, NV petrocalcic horizons: geomorphic and paleoenvironmental interpretations. Catena 77:65-75.

• Chesworth W, editor. 2008. Encyclopedia of soil science. Springer. 902 p.

• Dan J, Gerson R, Koyumdjisky H, Yaalon DH. 1981. Aridic soils of Israel. ARO Special publication, nº 19. Israel: Bet-Dagan. 353 p.

• Dorronsoro C, Alonso P. 1994. Chronosequence in Almar River fluvial-terrace soil. Soil Sci Soc Am J. 58:910-925.

• Durand N, Monger CH, Canti MG. 2010. Interpretation of Micromorphological Features of Soils and Regoliths. In: Stoops G, Vera M, Florias M, editors. Calcium Carbonate Features, Chapter 9. Amsterdam: Elsevier. p. 149-194.

• FAO. 2006. Guidelines for Soil Description. 4th edition. Rome: FAO. 97 p.

• Fedoroff N, Courty MA. 2012. Textural features and microfacies expressing temporary and permanent soil water saturation. In: Proceedings of the 14th International Working Meeting on Soil Micromorphology; 2012 July 8-14; Lleida, Spain; p. 7-10.

• Fedoroff N, Courty MA, Guo ZT. 2010. Palaeosoils and relict soils. In: Stoops G, Marcelino V, Mees F, editors. Interpretation of Micromorphological Features of Soils and Regoliths. Amsterdam: Elsevier. p. 623-662.

• Finke PA, Hutson, JL. 2008. Modelling soil genesis in calcareous loess. Geoderma 145:462-479.

• Gallardo JF, Pérez-González J, Almorox J. 2002. Secuencia de suelos sobre depósitos aluviales pliocenos y cuaternarios en el área de Talavera de la Reina: indicadores paleoclimáticos. In: Pérez-González A, Vegas J, Machado MJ, editors. Aportaciones a la geomorfología de España en el tercer milenio. Serie Geología, 1. Madrid: IGME. p.199-208.

• García-Castellanos D, Vergés J, Gaspar-Escribano J, Cloetingh S. 2003. Interplay between tectonics, climate, and fluvial transport during the Cenozoic evolution of the Ebro Basin (NE Iberia). Journal of Geophysical Research 108: 2347.

• Gee GW, Bauder JW. 1986. Particle-size analysis. In: Klute A, editor. Methods of Soil analysis. Part 1: Physical and Mineralogical methods. 2nd ed. Madison: American Society of Agronomy. p. 383-412.

• Gile LH, Peterson FF, Grossman RB. 1966. Morphological and genetic sequences of carbonate accumulation in desert soils. Soil Science 101:347-360.

• Gómez-Miguel V. 2005. Mapa de suelos de España (1:1.000.000). Atlas Nacional de España. Madrid: Instituto Geográfico Nacional.

• González-Sampériz P. 2004. Evolución paleoambiental del sector central de la Cuenca del Ebro durante el Pleistoceno Superior y Holoceno. Zaragoza: IPE-UZ. 210 p.

• González-Sampériz P, Leroy SAG, Carrión JS, Fernández S, García-Antón M, Gil-García MJ, Uzquinao P, Valero-Garcés B, Figueira I. 2010. Steppes, savannahs, forests and phytodiversity reservoirs during the Pleistocene in the Iberian Peninsula. Review of Palaeobotany and Palynology 162(3):427-457.

• Hamer JMM, Sheldon ND, Nichols GJ, Collinson ME. 2007. Late Oligocene-Early Miocene paleosols of distal fluvial systems, Ebro Basin, Spain. Palaeogeogragphy, Palaeoclimatology, Palaeoecology 247:220-235.

• Huggett RJ. 1998. Soil chronosequences, soil development, and soil evolution: a critical review. Catena 32:155-172.

• IUSS Working Group WRB. 2007. World Reference Base for Soil Resources 2006, first update. World Soil Resources Reports nº 103. Rome: FAO.

• Khormali F, Abtahi A, Mahmoodi S, Stoops G. 2003. Argillic horizon development in calcareous soils of arid and semiarid regions of southern Iran. Catena 53:273-301.

• Kooistra M, Pulleman MM. 2010. Features related to faunal activity. In: Stoops G, Mees F, Marcelino V, editors. Interpretation of Micromorphological features of Soils and Regoliths. Amsterdam: Elsevier. p. 397-419.

• Lequy E, Conil S, Turpault MP. 2012. Impacts of aeolian dust deposition on European forest sustainability: A review. Forest Ecology and Management 267:240-252.

• Lewis CJ, McDonald EV, Sancho C, Peña JL, Rhodes L, Edward J. 2009. Climatic implications of correlated Upper Pleistocene glacial and fluvial deposits on the Cinca and Gállego Rivers (NE Spain) based on OSL dating and soil stratigraphy. Global and Planetary Change 67(3-4):141-152.

• Machette MN. 1985. Calcic soils of the southwestern United States. In: Weide DL, editor. Soils and Quaternary geology of the southwestern United States. Geological Society of America, Special paper 203. p. 1-61.

• Markovic SB, Hambach U, Stevens T, Kukla GJ, Heller F, McCoy WD, Oches EA, Björn Buggle B, Zöller L. 2011. The last million years recorded at the Stari Slankamen (Northern Serbia) loess-palaeosol sequence: revised chronostratigraphy and long-term environmental trends. Quaternary Science Reviews 30(9-10):1142-1154.

• McLean EO. 1982. Soil pH and lime requirement. In: Page AL, Miller RH, Keeney DR, editors. Part 2: Chemical and Microbiological Properties. 2nd ed. Madison: American Society of Agronomy. p. 199-224.

• Meléndez A, Alonso-Zarza AM, Sancho C. 2011. Multistorey calcrete profiles developed during the initial stages of the configuration of the Ebro Basin's exorrheic fluvial network. Geomorphology 134:232-248.

• Mermut A, Pape T. 1971. Micromorphology of two soils from Turkey, with special reference to in-situ formation of clay cutans. Geoderma 5:271-281.

• Monger HC, Gile LH, Hawley JW, Grossman RB. 2009. The Desert Project: An Analysis of Arid land Soil-Geomorphic Processes. NMSU Agri. Exp. Station Bulletin 798. 76 p.

• Moreno A, González-Sampériz P, Morellón M, Valero-Garcés BL, Fletcher WJ. 2012. Northern Iberian abrupt climate change dynamics during the last glacial cycle: A view from lacustrine sediments. Quaternary Science Reviews 36:139-153.

• Nelson RE. 1982. Carbonate and gypsum. In: Page AL, Miller RH, Keeney D R, editors. Methods of Soil Analysis. Part 2: Chemical and Microbiological Properties 2nd ed. Madison: American Society of Agronomy. p. 181-198.

• Nelson RE, Sommers LE. 1982. Total carbon and organic matter. In: Page AL, Miller RH, Keeney DR, editors. Methods of soil analysis. Part 2: Chemical and microbiological properties. 2nd edition. Madison, Wisconsin: American Society of Agronomy. p. 539-557.

• Nettleton WD, Allen BL, Hallmark CT. 1991. Occurrence, characterization and genesis of carbonate, gypsum and silica accumulation in soils. SSSA Special Publication Number 26. Madison: Soil Science Society of America.

• Nettleton WD, Olson CG, Wysocki DA. 2000. Paleosol classification: Problems and solutions. Catena 41:61-92.

• Ortiz I, Simón M, Dorronsoro C, Martín F, García I. 2002. Soil evolution over the Quaternary period in a Mediterranean climate (SE Spain). Catena 48:131-148.

• Pazos MS. 1990. Some features and processes associated with the caliche under humid climate, Balcarce, Argentina. Pedologie XL-2:141-154.

• Poch RM, Simó I, Boixadera J. 2012. Benchmark soils on fluvial and fluvio-glacial formations of the upper-Segre valley. In: Proceedings of the 14th International Working Meeting on Soil Micromorphology; 2012 Jul 8-14; Lleida, Spain; p. 11-15.

• Quénard L, Samouëlian A, Laroche B, Cornu S. 2011. Lessivage as a major process of soil formation: A revisitation of existing data. Geoderma 167-168:135-147.

• Retallack GJ. 2005. Pedogenic carbonate proxies for amount and seasonality of precipitation in paleosols. Geology 33:333-336.

• Rhoades JD. 1982a. Soluble salts. In: Page AL, Miller RH, Keeney DR, editors. Methods of Soil Analysis. Part 2: Chemical and Microbiological Properties. 2nd edition. Madison: American Society of Agronomy. p. 167-180.

• Rhoades JD. 1982b. Cation exchange capacity. In: Page AL, Miller RH, Keeney, DR, editors. Methods of soil analysis. Part 2: Chemical and microbiological properties. 2nd edition. Madison: American Society of Agronomy. p. 149-158.

• Rodríguez J. 1986. Geomorfología de las Sierras Exteriores oscenses y su piedemonte. Colección de Estudios Altoaragoneses, nº 4. Huesca. 172 pp.

• Rodríguez R, Herrero J, Porta J. 1990. Micromorphological assessment of drain siltation risk indexes in a saline-sodic soil in Monegros irrigation district (Spain). In: Douglas LA, editor. Soil Micromorphology: A Basic and Applied Science. Issue 19. Amsterdam: Elsevier. p. 41-51.

• Roquero E, Goy JL, Zazo C. 1999. Fenómenos de convergencia genética en suelos de terrazas fluviales: Valle del río Tajo, Madrid-Toledo, España. Rev Soc Geol España 12(3-4):329-338.

• Sancho C, Muñoz A, González-Sampériz P, Osácar MC. 2011. Palaeoenvironmental interpretation of Late Pleistocene–Holocene morphosedimentary record in the Valsalada saline wetlands (Central Ebro Basin, NE Spain). Journal of Arid Environments 75(8):742-751.

• Sancho C, Peña JL, Muñoz A, Benito G, McDonald E, Rhodes EJ, Longares LA. 2008. Holocene alluvial morphopedosedimentary record and environmental changes in Bardenas Reales Natural Park (NE Spain). Catena 73:225-2328.

• Schultz LG. 1964. Quantitative interpretation of mineralogical composition from X-ray and chemical data for the Pierre Shale. US Geological Survey Professional Paper 391-C, C1-C31.

• Sheldon ND, Tabor NJ. 2009. Quantitative paleoenvironmental and paleoclimatic reconstruction using paleosols. Earth-Science Reviews 95:1-52.

• Soil Survey Staff. 2010. Keys to Soil Taxonomy. 10th edition. Washington: USDA-Natural resources Conservation Service.

• Wilson MJ. 1999. The origin and formation of clay minerals in soils: past, present and future perspectives. Clay Minerals 34:7-25.

• Zielhofer C, Recio Espejo JM, Núñez Granados MA, Faust D. 2009. Durations of soil formation and soil development indices in a Holocene Mediterranean floodplain. Quaternary International 209:44-65.